Selected for a Viewpoint in *Physics*

Coherent Terahertz Sound Amplification and Spectral Line Narrowing in a Stark Ladder Superlattice

R. P. Beardsley, A. V. Akimov, M. Henini, and A. J. Kent

School of Physics and Astronomy, University of Nottingham, University Park, Nottingham NG7 2RD, United Kingdom
(Received 15 October 2009; published 22 February 2010)

The bias voltage applied to a weakly coupled *n*-doped GaAs/AlAs superlattice increases the amplitude of the coherent hypersound oscillations generated by a femtosecond optical pulse. This bias-induced amplitude increase and experimentally observed spectral narrowing of the superlattice phonon mode with a frequency 441 GHz provides the evidence for hypersound amplification by stimulated emission of phonons in a system where the inversion of the electron populations for phonon-assisted transitions exists.

DOI: 10.1103/PhysRevLett.104.085501 PACS numbers: 63.20.kd, 63.22.Np, 72.80.Ey, 73.21.Cd

The methods of coherent terahertz (THz) acoustics developed during the last decade offer new possibilities for extending the techniques of traditional ultrasonics to much higher frequencies where they can be applied to electronics, photonics and the studies of nanoscale systems. Generation and detection of coherent elastic waves with THz frequency have been successfully realized in a number of nano-objects, especially semiconductor superlattices (SLs) [1–6]. Currently, significant effort is aimed at developing THz acoustic analogues of active optical devices like lasers and amplifiers. The THz acoustic nanodevices (e.g., saser) based on the sound amplification by stimulated emission of acoustic radiation in combination with phonon microcavities [7] will provide a source of an intense beam of coherent sound and have the potential to transform hypersonic acoustics in a similar way to how the laser transformed optics.

A few methods for GHz–THz sound amplification have been proposed. Some have so far been explored only theoretically [8,9] and others have been explored only in noncoherent experiments [10,11]. In order to obtain much stronger evidence for coherent sound amplification by stimulated phonon emission, it is essential to use a detection technique that is sensitive to the coherent nature of the acoustic modes.

In the present Letter we report coherent ultrafast acoustic experiments in a doped semiconductor SL under applied electrical bias. If the SL is biased such that the energy drop per period of the SL exceeds the width of electronic minibands (Wannier-Stark regime), the electrons become localized in the quantum wells (QWs) and vertical electron transport takes place via hopping between neighboring QWs which may be phonon assisted [12]. It had previously been theoretically predicted [13,14] and subsequently shown experimentally [10,15] that, under these conditions, stimulated phonon emission [Fig. 1(a)] can be the dominant phonon-assisted hopping process for phonons of a particular energy close to the Stark splitting, and so coherent phonon amplification is theoretically possible in this system. The main aim of the present experiments is to show whether the THz stimulated phonon induced transitions between the electron SL states possessing an inversion population can lead to the *coherent* amplification of THz sound.

The sample [Fig. 1(c)] used was a 50-period GaAs/AlAs SL grown by molecular beam epitaxy on a 0.4 mm-thick semi-insulating GaAs substrate. Each period consisted of a

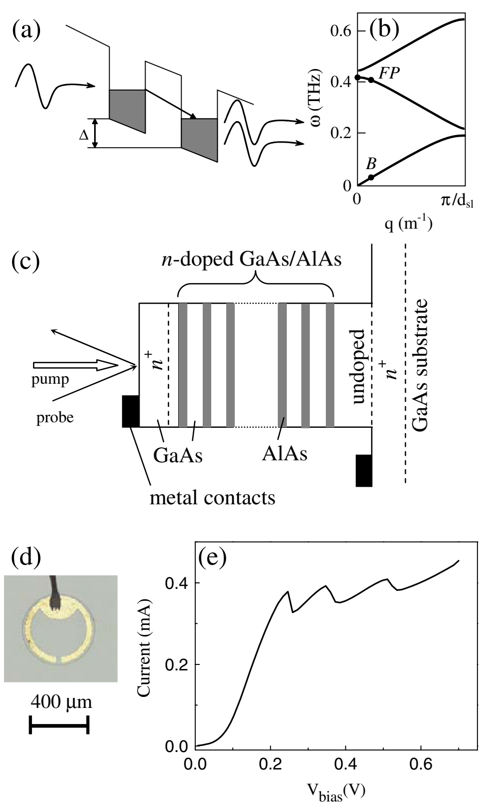

FIG. 1 (color online). (a) Schematic representation of phonon-assisted tunneling between neighboring QWs in the SL by stimulated emission; (b) folded LA phonon dispersion in a GaAs/AlAs SL with a period $d_{SL} = 10$ nm, the Brillouin backscattering, *B*, and folded phonon, *FP*, modes are indicated; (c) the structure of the experimental device; (d) photograph of the optical MESA structure and (e) device current-voltage characteristics (negative bias to top contact).

5.9 nm-thick GaAs QW and a 3.9 nm-thick AlAs barrier, uniformly n doped with Si to a density of 2×10^{16} cm^{-3}. The SL was separated from the n^+ (2×10^{18} cm^{-3}) contact regions by 20 nm-thick undoped GaAs spacer layers. This structure was chosen as it is close to the optimum for observing phonon amplification and had previously shown evidence of it in nonequilibrium phonon measurements [10,15]. A 400 μm-diameter optical device mesa was formed by etching and contacts with the emitter and collector layers were made using InGeAu, annealed at 360 °C. The top contact was etched in a form of a ring [Fig. 1(d)] leaving a metal free region for optical excitation. Measurements were made at 10 K in order to reduce the thermal background such that $k_B T < \hbar\omega$ for phonons of frequency ω. The dc current-voltage (I-V) characteristics are shown in Fig. 1(e). In the dark, the device turns on at the threshold bias 50 mV, which is the voltage required to align the Fermi energy of the emitter and the nearest well. After that, the current increases monotonically for biases up to about 250 mV. The illumination of the device by light of wavelength $\lambda = 773$ nm which corresponds to the SL electron-hole resonance (1.6 eV), with an average power $\sim$10 mW, led to a decrease in the threshold to about 30 mV and a small increase in the current, otherwise the I-V characteristics were much the same as in the dark.

The coherent phonon measurements were carried out using the femtosecond pump-probe technique: owing to the difference in the acoustic impedance of the two semiconductors making up the SL, narrow gaps open up in the phonon dispersion at wave vectors $\mathbf{q}$ corresponding to the Bragg reflection of sound in the periodic structure [Fig. 1(b)]. Coherent folded phonons (FPs) in the narrow frequency bands with energies close to the gaps in the phonon dispersion can be generated by femtosecond laser excitation of the SL sample using a wavelength near the electron-hole resonance [1–6]. Coherent detection of the FPs is achieved by measuring the change in reflectance, $\Delta R(t)$, for a femtosecond probe pulse as a function of the delay time t between the pump and probe pulses. In these experiments, the delay was provided by two (shaker and motorized) optical delay lines in the pump beam path and one (manual) delay line in the probe path. The shaker delay was a retroreflector mounted on a platform vibrating with a frequency 2.5 Hz and linear distance amplitude up to 8.25 mm providing the measurements in the temporal interval up to 50 ps. The motorized and manual delay lines were used to fix the center delay time t_0 with precision of $\sim$1 ps, around which the measurement using the shaker were taken. The pump beam was modulated at a frequency of 50 kHz by an acousto-optic modulator and the reflected probe beam was detected by a photodiode followed by a lock-in amplifier referenced to the pump modulation. The output of the lock-in amplifier was connected to the input of a digital averaging oscilloscope which was triggered from the shaker delay line. This experimental setup enabled measurement for temporal delays up to 3 ns of the values of temporal changes in the reflectance as small as $\Delta R(t)/R_0 \sim 10^{-7}$, where R_0 is the reflectance in the absence of the pump pulse.

Figure 2 shows a typical probe signal $\Delta R(t)/R_0$ at $V_{\mathrm{bias}} = 0$ in the temporal range 0–450 ps. The main contribution at $t > 0$ is due to the nonequilibrium carriers excited by the pump pulse. This contribution is considered as a background for the coherent sound signal and it is often subtracted for the clarity of presentation. The zoomed section of the measured $\Delta R(t)$ [inset in Fig. 2] clearly shows oscillatory behavior with low (45 GHz) and high (0.441 THz) frequencies. The low-frequency B mode is attributed to the Brillouin backscattering effect and it is observed in $\Delta R(t)$ only in the time interval between 100 and 300 ps. This interval corresponds to the time when the coherent low-frequency (<100 GHz) wave packet generated by the pump pulse in the near surface GaAs region [16] of the sample [Fig. 1(c)] reaches the superlattice where the sensitivity of the probe light to the strain significantly exceeds the sensitivity of surrounding bulk GaAs layers [17]. The high frequency oscillations are known to be associated with the FPs near the first gap in the Γ point of the phonon dispersion curves in the GaAs/AlAs SL [Fig. 1(b)].

Application of a bias to the SL led to an increase in the amplitude of the FPs. This can be seen by comparison of the Fourier transforms in a 50 ps window centered on $t_0 =$ 1 ns at zero bias and at $V_{\mathrm{bias}} = 145$ mV, Fig. 3. This is the first strong indication that amplification of coherent phonons takes place under bias application. The significant increase of amplitude was observed for bias values above about 120 mV (see inset to Fig. 3) which, after taking account of the threshold, corresponds to a Stark splitting of about 1.8 meV. The energy of the FPs excited in the SL is also about 1.8 meV; thus, the amplification occurs for Stark splittings which are larger than this, which is the condition under which inversion is predicted to occur [13,14].

The observed increase in the signal is about 40% which is reasonable in view of estimates of the phonon densities: based on a measured strain of $\sim 10^{-6}$, the density of laser generated longitudinal FPs is 2.5×10^{20} m^{-3} at 440 GHz.

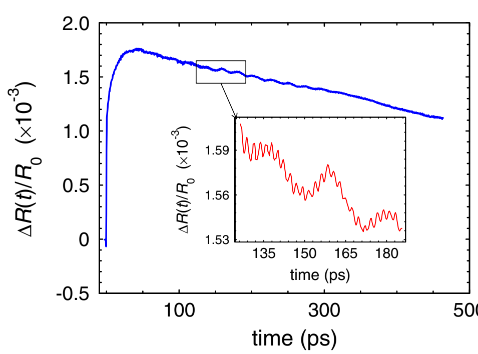

FIG. 2 (color online). Time evolution of the reflectivity changes $\Delta R(t)$ at zero bias. The inset shows a fragment of the time evolution for $\Delta R(t)$ in which the oscillations due to the FP modes are clearly seen.

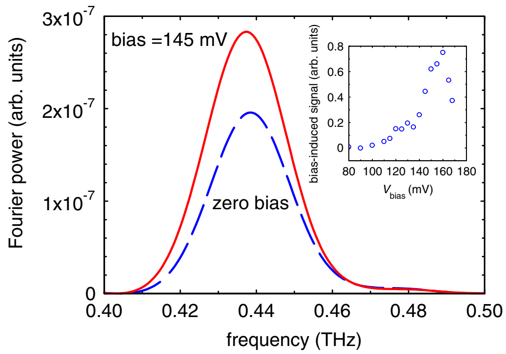

FIG. 3 (color online). Fourier spectra of the FP mode in a 50 ps window centered on $t_0 = 1$ ns for zero bias and a constant bias of 145 mV. The inset shows the bias-induced signal change at the peak (compared to the peak at zero bias) as a function of the applied bias voltage.

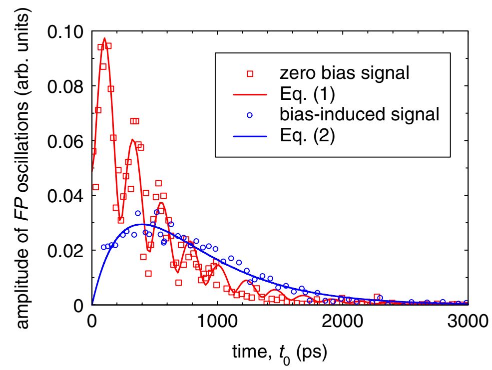

FIG. 4 (color online). The amplitude of the FP oscillations at zero bias (squares) and the amplitude of the bias-induced oscillations (circles). The solid lines are, respectively, the fits of Eqs. (1) and (2) to the data.

The thermal background longitudinal phonon density at $T = 10$ K is 2.5×10^{21} m^{-3} in a 1 GHz band at 440 GHz. However, only those phonons with wave vector direction within about 5° of the SL normal can be amplified [15]. This applies to nearly all the laser generated FPs, but only 0.2% of the thermal phonons. Therefore, with regard to amplification by stimulated emission, the laser generated phonons are dominant. The current density in the SL at a bias of 145 mV is about 800 Am^2, which means that in about 0.5 ns, which is the approximate lifetime of the phonons in the SL, there are $\sim 10^{14}$ electron "hops" per m^2. If every hop was due to stimulated emission, this would result in the phonon density increase of about 2×10^{20} m^{-3}, similar to the laser induced density. So, even if every electron hop was due to a stimulated phonon emission, we should expect no more than a ~100% increase in signal. This estimate assumes the phonons are generated throughout the entire SL, which is reasonable if we assume a typical 2% absorption of the pump light per QW.

Of course, there remains the possibility that the observed increase of amplitude is not due to amplification of a phonon mode, but is instead due to changes in the efficiency of the coherent phonon generation and/or detection process caused by application of the bias. The fact that the amplitude of the B mode was not increased upon application of bias tends to rule out any change in detection sensitivity. However, to properly address this question, the effect of applied bias on the spectrum of the oscillations was studied. It is expected that the process of amplification by stimulated emission would lead to spectral narrowing, whereas a change in the sensitivity should not. In order to obtain sufficient spectral resolution it was necessary to measure for delay times in excess of 1 ns. This could not be done with sufficient sensitivity and temporal resolution in a single sweep. Instead, using the shaker delay, 50 ps fragments were recorded with high sensitivity centered on time delays, t_0, up to 3 ns. These were Fourier transformed to give the amplitude of the high frequency oscillations as a function of t_0. Figure 4 shows the envelope of the amplitude of the FPs at zero bias. It is seen that the amplitude decays on the time scale of about 0.5 ns, also obvious are the oscillations in the amplitude with a period of about 220 ps. These oscillations are likely to be due to the beating of two modes with a difference in frequency of about 4.5 GHz. The solid line is a fit to the data of the analytical expression representing two beating cosine waves of amplitudes ratio B and frequency difference $\Delta\nu$:

$$F(t_0) = A_0 \exp(-\gamma_0 t_0)[1 + B^2 + 2B\cos(2\pi\Delta\nu t_0)]^{1/2}, \quad (1)$$

where $\gamma_0 = (2.1 \pm 0.1)\,\text{ns}^{-1}$, $B = (-0.43 \pm 0.03)$, $|\Delta\nu| = (4.5 \pm 0.03)$ GHz, and A_0 is a normalization factor. The spectrum of the coherent phonons, shown in Fig. 5, is obtained by taking the analytical Fourier transform of Eq. (1). To identify the frequencies of the two lines, we used the direct measurements of $\Delta R(t)/R_0$ at $V_{bias} = 0$ in a wide temporal range (Fig. 1). These measurements allowed us to identify that the higher amplitude mode has a frequency of 0.4410 THz. The weaker mode at 0.4365 THz [18] is too close in frequency to be one of the backscattering modes at $2k_{laser}$, and probably arises due to the finite length of the SL [19]. This gives rise to quantization of the acoustic dispersion into modes separated by $\Delta\nu \approx s/2L$, where L is the SL length. In this case $L = 0.5$ μm, which gives $\Delta\nu \approx 5$ GHz which, if allowance is made for the flattening of the

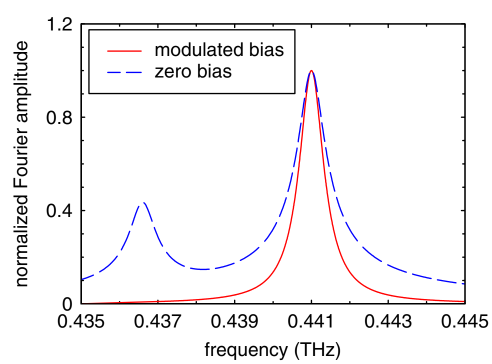

FIG. 5 (color online). The spectra of the FP modes at zero bias and the bias-induced signal.

acoustic dispersion as $q \to 0$, is close to the experimentally measured value.

Also shown in Fig. 4 is the envelope of the difference between the bias on and zero-bias signals, i.e., the additional signal due to the applied bias. In order to obtain this with high sensitivity and low background noise, the pump modulation was switched off and the bias was modulated between 0 V and V_{bias} at a frequency of 50 kHz. Otherwise the same pump-probe scheme was used as at zero bias. The most striking feature of this result is the absence of the beating which implies that only one of the two modes observed at zero bias is increased by amplification. There is also evidence of a buildup of amplitude of the mode occurring at shorter times. Such a buildup of amplitude is expected for the dynamical response in the regime of amplification [20]. As before, to obtain the spectrum of the acoustic oscillations, we fit the following analytical expression to the difference signal

$$F(t_0) = A_1 \exp(-\gamma_1 t_0)[1 - \exp(-g t_0)], \qquad (2)$$

where $\gamma_1 = (2.0 \pm 0.1)\ \mathrm{ns}^{-1}$, $g = (0.9 \pm 0.3)\ \mathrm{ns}^{-1}$, and A_1 is a normalization factor. The spectrum obtained by taking the Fourier transform of Eq. (2) is shown in Fig. 5. The amplitude spectrum of the bias-induced oscillations is significantly narrower than that of the zero-bias FPs. Taking into account the errors in the fitting parameters above gives a maximum 10% error in the difference between the line widths, which is smaller than the observed narrowing. This result provides strong evidence for acoustic amplification by stimulated phonon emission occurring in the system. However, the amount of narrowing is much less than is typical in optical amplifiers. The probable reason for this is that the decay of the FP oscillations is dominated by the effects of dephasing due to submonolayer thickness fluctuations across the probed area [21], rather than by phonon escape from the SL.

To conclude, application of an electrical bias to a weakly coupled semiconductor superlattice gives rise to an increase in the amplitude of the coherent folded phonons generated by a femtosecond optical pulse. The increase of amplitude is observed for biases such that the energy drop per period of the superlattice is greater than the phonon energy. As well as the increase in amplitude, the spectrum of the bias-induced oscillations is narrower than the spectrum of the coherent phonons at zero bias. These results show that coherent amplification of phonons due to stimulated emission takes place in the structure under electrical pumping. The achievement of amplification for coherent THz sound provides an essential step towards coherent generation (sasing) of THz sound and other active hypersound devices. In a device where the threshold for sasing is achieved, the technique described here could be used to measure the coherence time of the emitted hypersound. In this case, the effect of the pump would be to phase-lock the oscillation and the dephasing time determined using measurements of the decay of the oscillations as a function of the probe delay.

The authors acknowledge support for this work from EPSRC of the U.K. and the Royal Society, and also valuable discussions with Dr. Boris Glavin.

[1] A. Yamamoto, T. Mishina, Y. Masumoto, and M. Nakayama, Phys. Rev. Lett. **73**, 740 (1994).
[2] A. Bartels, T. Dekorsy, H. Kurz, and K. Kohler, Phys. Rev. Lett. **82**, 1044 (1999).
[3] K. Mizoguchi, M. Hase, S. Nakashima, and M. Nakayama, Phys. Rev. B **60**, 8262 (1999).
[4] C-K Sun, J-C Liang, and X-Y Yu, Phys. Rev. Lett. **84**, 179 (2000).
[5] E. Makarona, B. Daly, J.-S. Im, H. Maris, A. Nurmikko, and J. Han, Appl. Phys. Lett. **81**, 2791 (2002).
[6] M. Trigo, T. A. Eckhause, M. Reason, R. S. Goldman, and R. Merlin, Phys. Rev. Lett. **97**, 124301 (2006).
[7] A. Huynh, N. D. Lanzillotti-Kimura, B. Jusserand, B. Perrin, A. Fainstein, M. F. Pascual-Winter, E. Peronne, and A. Lemaître, Phys. Rev. Lett. **97**, 115502 (2006).
[8] S. M. Komirenko, K. W. Kim, A. A. Demidenko, V. A. Kochelap, and M. A. Stroscio, Phys. Rev. B **62**, 7459 (2000).
[9] S. S. Makler, M. I. Vasilevsky, E. V. Anda, D. E. Tuyarot, J. Weberszpil, and H. M. Pastawski, J. Phys. Condens. Matter **10**, 5905 (1998).
[10] A. J. Kent, R. N. Kini, N. M. Stanton, M. Henini, B. A. Glavin, V. A. Kochelap, and T. L. Linnik, Phys. Rev. Lett. **96**, 215504 (2006).
[11] L. G. Tilstra, A. F. M. Arts, and H. W. de Wijn, Phys. Rev. B **76**, 024302 (2007).
[12] R. Tsu and G. Dohler, Phys. Rev. B **12**, 680 (1975).
[13] B. A. Glavin, V. A. Kochelap, and T. L. Linnik, Appl. Phys. Lett. **74**, 3525 (1999).
[14] B. A. Glavin, V. A. Kochelap, T. L. Linnik, K. W. Kim, and M. A. Stroscio, Phys. Rev. B **65**, 085303 (2002).
[15] R. N. Kini, A. J. Kent, N. M. Stanton, and M. Henini, J. Appl. Phys. **98**, 033514 (2005).
[16] O. B. Wright, B. Perrin, O. Matsuda, and V. E. Gusev, Phys. Rev. B **64**, 081202(R) (2001).
[17] A. V. Akimov, A. V. Scherbakov, D. R. Yakovlev, C. T. Foxon, and M. Bayer, Phys. Rev. Lett. **97**, 037401 (2006).
[18] It is not possible to deduce from Fig. 4 whether the weaker mode is at a frequency above or below the stronger one. On the assumption that the stronger mode occurs where the lower branch of the folded dispersion reaches $q = 0$ [2] at a frequency of 441 GHz, then the weaker mode is more likely to be at a lower frequency where it lies on the folded dispersion curve rather than at a higher frequency where it would be in the gap. However, it does not materially affect the main conclusion of this work whether the weaker mode is at a higher or lower frequency.
[19] M. W. C. Dharma-wardana, P. X. Zhang, and D. J. Lockwood, Phys. Rev. B **48**, 11 960 (1993).
[20] O. Svelto, *Principles of Lasers* (Springer, New York, 2005), 4th ed., ISBN 978-0-306-45748-7.
[21] G. Rozas, M. F. Pascual Winter, B. Jusserand, A. Fainstein, B. Perrin, E. Semenova, and A. Lemaître, Phys. Rev. Lett. **102**, 015502 (2009).